J Membrane Biol (2007) 216:73–82
DOI 10.1007/s00232-007-9034-z

Mechanism of Interaction of Niflumic Acid with Heterologously Expressed Kidney CLC-K Chloride Channels

Alessandra Picollo · Antonella Liantonio · Elena Babini · Diana Conte Camerino · Michael Pusch

Received: 19 October 2006 / Accepted: 8 May 2007 / Published online: 21 July 2007

Abstract CLC-K Cl^- channels belong to the CLC protein family. In kidney and inner ear, they are involved in transepithelial salt transport. Mutations in ClC-Kb lead to Bartter's syndrome, and mutations in the associated subunit barttin produce Bartter's syndrome and deafness. We have previously found that 3-phenyl-CPP blocks hClC-Ka and rClC-K1 from the extracellular side in the pore entrance. Recently, we have shown that niflumic acid (NFA), a nonsteroidal anti-inflammatory fenamate, produces biphasic behavior on human CLC-K channels that suggests the presence of two functionally different binding sites: an activating site and a blocking site. Here, we investigate in more detail the interaction of NFA on CLC-K channels. Mutants that altered block by 3-phenyl-2-(p-chlorophenoxy)propionic acid (CPP) had no effect on NFA block, indicating that the inhibition binding site of NFA is different from that of 3-phenyl-CPP and flufenamic acid. Moreover, NFA does not compete with extracellular Cl^- ions, suggesting that the binding sites of NFA are not located deep in the pore. Differently from ClC-Ka, on the rat homologue ClC-K1, NFA has only an inhibitory effect. We developed a quantitative model to describe the complex action of NFA on ClC-Ka. The model predicts that ClC-Ka possesses two NFA binding sites: when only one site is occupied, NFA increases ClC-Ka currents, whereas the occupation of both binding sites leads to channel block.

A. Picollo · E. Babini · M. Pusch (✉)
Istituto di Biofisica,
CNR, Via De Marini, 6, I-16149 Genoa, Italy
e-mail: pusch@ge.ibf.cnr.it

A. Liantonio · D. C. Camerino
Unità di Farmacologia, Dipartimento Farmacobiologico,
Facoltà di Farmacia, Università di Bari, Via Orabona, 4,
1-70125 Bari, Italy

Keywords CLC-K channel · Niflumic acid · Flufenamic acid

Introduction

The CLC Cl^- channels ClC-Ka and ClC-Kb are two human, highly homologous isoforms (Kieferle et al., 1994). In rodents, these two isoforms are called ClC-K1 and ClC-K2 (Adachi et al., 1994). Probably, ClC-Ka corresponds to ClC-K1, whereas ClC-Kb is the species homologue of ClC-K2. Within a single species the two isoforms are 90% identical in their primary structure. The high degree of homology is probably caused by a relatively recent gene duplication as both genes are located on human chromosome 1p36 (Brandt & Jentsch, 1995) and are separated by only 11 kb of genomic DNA (Simon et al., 1997). They are selectively expressed in the kidney and in the inner ear, where they are important for transepithelial salt transport. In the kidney, ClC-K1 is expressed in the thin ascending limb of Henle's loop and is thought to be one major determinant of the efficiency of urinary concentration (Matsumura et al., 1999). In contrast, ClC-K2 is localized in the thick ascending limb of Henle's loop and in other distal nephron segments (Adachi et al., 1994; Kieferle et al., 1994; Uchida & Sasaki, 2005; Vandewalle et al., 1997). In the inner ear, both channel isoforms are expressed in the stria vascularis, where they are implicated in the production of K^+-rich endolymph (Estévez et al., 2001). The relevance of these proteins is illustrated by genetic disorders. Mutations in the gene coding for ClC-Kb lead to Bartter's syndrome, a disease characterized by severe salt wasting and hypokalemia (Simon et al., 1997), whereas mutations in the small essential CLC-K channel subunit barttin lead to Bartter's syndrome and deafness (Birkenhäger et al., 2001). A few years ago, the barttin protein was

identified as a β-subunit that is necessary for the functional expression of CLC-K channels (Estévez et al., 2001). The identification of barttin has allowed the functional heterologous expression of CLC-K channels and exploration of their pharmacological properties. Small molecule ligands may be useful tools and possible drug candidates in various pathological situations (Fong, 2004).

A structure-activity study allowed us to identify a compound, 3-phenyl-CPP, with a chlorophenoxy group and an aromatic ring, able to block ClC-K1 and ClC-Ka currents. Interestingly, the highly homologous ClC-Kb channel is fivefold less sensitive to 3-phenyl-CPP compared to ClC-Ka (Picollo et al., 2004). We identified the amino acid residues responsible for this different drug sensitivity that probably make up part of the drug-binding site. In particular, asparagine N68 in ClC-Ka, located in helix B, plays a critical role in the blocking activity of 3-phenyl-CPP (Picollo et al., 2004). Very recently, Liantonio et al. (2006) demonstrated that ClC-Ka has also an activating binding site. Niflumic acid (NFA), a drug belonging to the class of fenamates and used as a nonsteroidal anti-inflammatory drug, increases ClC-Ka and ClC-Kb currents for concentrations in the 50–1,000 μM range. Instead, high concentrations (2–2.5 mM) of NFA blocked ClC-Ka currents (Liantonio et al., 2006). The biphasic concentration-response relationship of NFA measured for ClC-Ka evokes several questions. First, are there one or two distinct NFA-binding sites on the channel protein? Second, do NFA and the blocker 3-phenyl-CPP bind to the same site(s)? Third, is the NFA bind site(s) located in the inner pore? To answer these questions, in the present study, we used several approaches to investigate the mechanism with which NFA interacts with CLC-K channels. We demonstrate that the blocker-binding site of NFA is different from that of 3-phenyl-CPP. Moreover, we develop an experimental protocol to study separately the potentiation and inhibition effects of NFA on ClC-Ka. Our data are well described by a model in which there are two binding sites for NFA. If NFA binds to one of the two sites, CLC-K current amplitude is increased, whereas if NFA binds simultaneously to both sites, the channel is blocked.

The ability of NFA to open and to block CLC-K channels makes it a good starting point for identification of diuretics or drugs useful in the treatment of Bartter's syndrome type III.

Materials and Methods

Expression in Xenopus laevis Oocytes and Voltage-Clamp Analysis

Wild-type (WT) ClC-Ka (human), ClC-K1 (rat) and its mutant ClC-K1$_{N68D}$, obtained as previously described (Picollo et al., 2004), were coexpressed with mutant Y98A of human barttin, leading to enhancement of expression (Estévez et al., 2001). Expression in oocytes and electrophysiological measurements were performed as previously described (Pusch et al., 2000). Voltage-clamp data were acquired at room temperature (21–25°C) using a custom acquisition program (GePulse) and a TEC03 amplifier (npi electronic, Tamm, Germany). Currents were recorded in a standard solution containing (in mM) 90 NaCl, 10 $CaCl_2$, 1 $MgCl_2$, 10 4-(2-hydroxyethyl)-1-piperazineethanesulfonic acid (HEPES) at pH 7.3. In experiments with low extracellular chloride concentration, 90 mM NaCl was replaced with 180 mM sucrose.

To evaluate the current-voltage relationship, the voltage-clamp pulse protocol was as follows: from a holding potential of –30 mV, after a prepulse to 60 mV for 100 ms, voltage was stepped from –140 to 80 mV in 20-mV increments for 200 ms, followed by a final tail pulse to –100 mV. To evaluate the onset and washout of drug effects, a pulse to 60 mV was applied every 2 s. Solutions were applied under continuous perfusion. We noted that under continuous perfusion the absolute effects of NFA at 500 μM and 1 mM were slightly different compared to the data published earlier (Liantonio et al., 2006), which were obtained without continuous perfusion. The differences are relatively small; nevertheless, we regard the current data obtained under continuous perfusion as more reliable.

Data Analysis

To estimate the contribution of endogenous currents, we used the following strategy. We applied a solution containing 100 mM I^-, which blocks currents carried by CLC-K channels but not endogenous currents, and used the residual current in 100 mM I^- to estimate the contribution of endogenous currents (Picollo et al., 2004). These leak currents were subtracted from the control currents in the absence and presence of a drug, to obtain a correct estimation of CLC-K currents.

Apparent dissociation constants, K_d, for NFA and 3-phenyl-CPP (for rClC-K1 and rClC-K1$_{N68D}$) were determined by calculating the ratio of the steady-state currents in the presence and absence of the drug and fitting the ratios using a Langmuir isotherm:

$$\frac{I_{drug}}{I_{control}} = \frac{1}{1 + \left(c/K_d\right)^{\gamma}} \quad (1)$$

where c is the drug concentration and γ is the Hill coefficient. Errors in the figures and text are indicated as standard errors of the mean (SEM). Data points represent the average of at least three oocytes.

The perfusion protocol and the procedure to separate NFA-mediated block and potentiation are described in detail in the Results section. The initial current immediately after washout (I_2) was obtained by back-extrapolation of a single-exponential fit to the decaying current phase (see Fig. 6).

NFA, flufenamic acid (FFA) and all other reagents were purchased from Sigma-Aldrich (Milan, Italy). NFA, FFA and 3-phenyl-CPP were dissolved in dimethyl sulfoxide (DMSO), leading to a final maximal concentration of 0.05% DMSO. At this concentration, DMSO by itself had no effect on ClC-Ka-mediated currents and no effect on membrane currents of water-injected oocytes. Also, NFA at 200 μM had no effect on water-injected oocytes (*data not shown*). Because washout of NFA-mediated potentiation was relatively slow (several minutes), we discarded oocytes after having applied NFA at a particular concentration. Thus, the experiments illustrated below are from unpaired oocytes. This strategy was adopted also to exclude unrelated long-term effects that may have been caused by effects of NFA on cyclooxygenases.

Results

Effect of NFA on ClC-K1

NFA (Fig. 1A) is a known blocker of many Cl^- and other channels (Gögelein et al., 1990; Lee & Wang, 1999; McCarty et al., 1993; Qu & Hartzell, 2000; White & Aylwin, 1990). Previously, we tested NFA on heterologously expressed CLC-K channels and found that it inhibits rat ClC-K1 currents when applied at 200 μM (Liantonio et al., 2004). More recently, we showed that NFA has biphasic behavior on human ClC-Ka and ClC-Kb channels: low concentrations of NFA (50–500 μM) activate ClC-Ka, but higher concentrations (1–2 mM) block the channel (Liantonio et al., 2006). Because in the earlier experiments (Liantonio et al., 2004) NFA was applied only at a single concentration (200 μM) on ClC-K1, in the first series of experiments we tested different concentrations of NFA on ClC-K1 to find out if it has a biphasic effect also on the rat channel. As ClC-Ka, ClC-K1 partially deactivates at positive potentials and activates at negative potentials (Fig. 1B, left). The >60% block seen after application of 200 μM NFA is illustrated in Figure 1B (right). In contrast to ClC-Ka, we observed that NFA blocked ClC-K1 currents at all concentrations tested (10 μM–1 mM). The concentration-response curve is well fitted by a Langmuir isotherm equation with a Hill coefficient equal to 1 (Fig. 1C). This indicates that the inhibition produced by NFA on ClC-K1 can be well described by a simple 1:1 binding, resulting in the apparent K_d of 94 ± 17 μM.

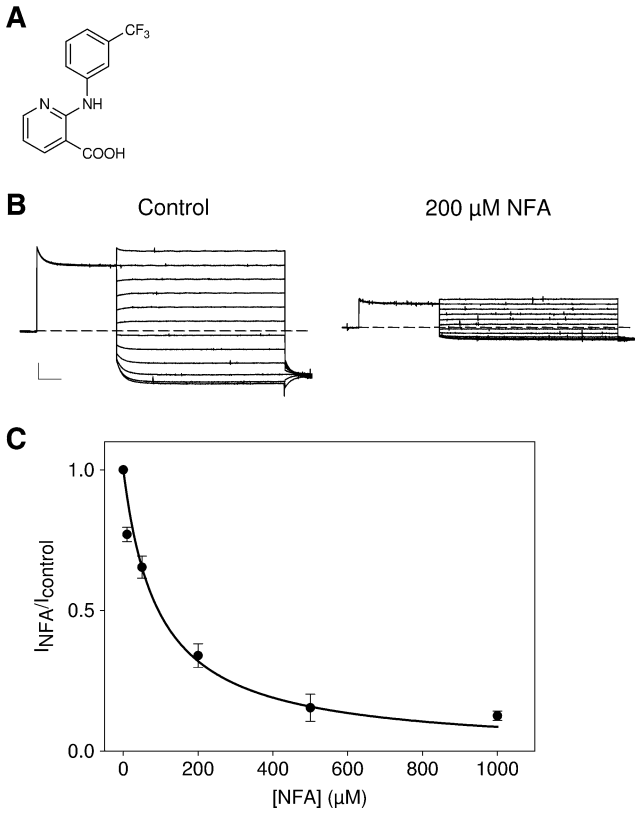

Fig. 1 Effect of NFA on ClC-K1. (**A**) Chemical structure of NFA. (**B**) Voltage-clamp traces of ClC-K1 currents before (*left*) and during application of 200 μM of NFA (*right*). Horizontal scale bar = 25 ms, vertical scale bar = 2 µA. (**C**) Concentration-response relationship of inhibition by NFA for ClC-K1. The ratio of the current in the presence and absence of drug is plotted *vs.* NFA concentration. The line is drawn according to the equation $I_c/I_0 = 1/(1 + c/K_d)$, with the apparent K_d value equal to 94 μM

Because ClC-K1 and ClC-Ka are highly homologous, it is reasonable to assume that the blocking site for NFA on ClC-K1 is identical, or at least very similar to the NFA-blocking site on ClC-Ka. Therefore, using ClC-K1 allowed us to investigate in more detail the properties of the NFA-blocking binding site, without interference from NFA-induced potentiation. In particular, we investigated the relationship of the NFA inhibitory site with the previously characterized inhibitory site for 3-phenyl-CPP (Picollo et al., 2004). We had identified several crucial amino acids involved in the inhibitory binding site of 3-phenyl-CPP (Picollo et al., 2004). Because NFA, as 3-phenyl-CPP, is negatively charged at physiological pH, we tested if the blocking site of NFA is equivalent to that of 3-phenyl-CPP. In particular, we verified if residue 68 is involved in the binding site of NFA. This neutral residue (asparagine) is conserved among ClC-K1 and ClC-Ka. In ClC-Ka, amino acid 68 performs a critical role in the binding of 3-phenyl-CPP (Picollo et al., 2004). The introduction of a negative charge ($ClC\text{-}Ka_{N68D}$) in this position renders ClC-Ka more

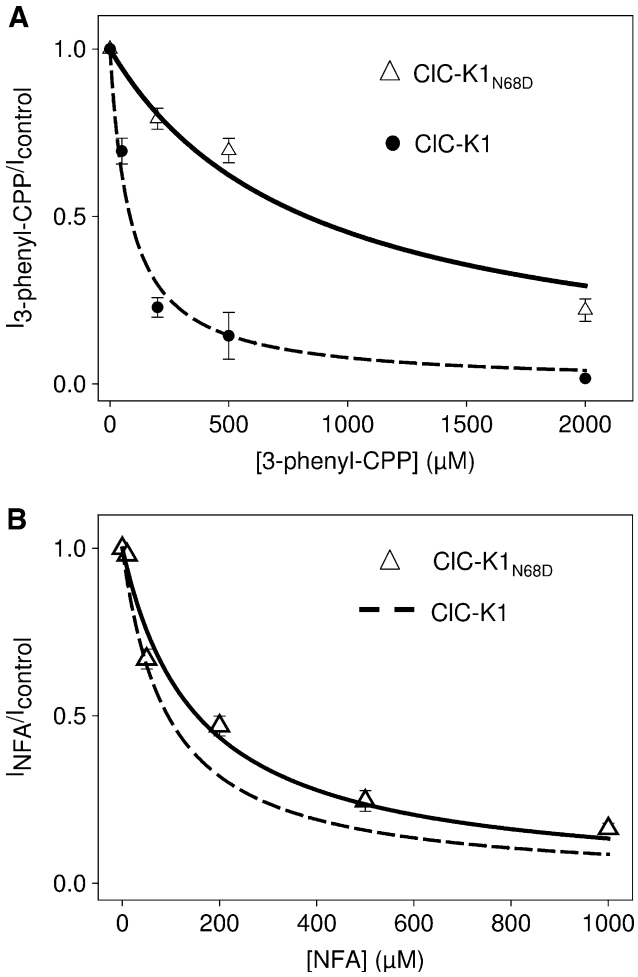

Fig. 2 Inhibition by 3-phenyl-CPP (**A**) and NFA (**B**) of ClC-K1 and ClC-K1$_{N68D}$. The ratio of currents in the presence and absence of drugs is plotted *vs.* drug concentration. Lines are drawn according to equation 1. 3-Phenyl-CPP has a K_d of 84 and 824 μM for ClC-K1 and ClC-K1$_{N68D}$, respectively. NFA has a K_d of 94 μM and 156 for μM ClC-K1 and ClC-K1$_{N68D}$, respectively. *Dashed line* in **B** represents the fit to the WT data shown in Figure 1C

than fivefold less sensitive to 3-phenyl-CPP (Picollo et al., 2004). As in ClC-Ka, the corresponding mutation in ClC-K1 (ClC-K1$_{N68D}$) is less sensitive to 3-phenyl-CPP compared with ClC-K1 (Fig. 2A). Fitting equation 1 with a Hill coefficient of 1 resulted in an apparent K_d for 3-phenyl-CPP >10-fold different in the mutant compared to WT ClC-K1 (84 μM for ClC-K1 compared to 828 μM for the N68D mutant). This result confirms that a neutral residue in position 68 is important for the block produced by 3-phenyl-CPP also for ClC-K1. Instead, NFA produced only a slightly smaller effect on ClC-K1$_{N68D}$ with respect to WT (Fig. 2B). Again, fitting equation (1) reveals a change in the apparent K_d of less than twofold (94 μM for ClC-K1 [dashed line in Fig. 2B, taken from Fig. 1C] and 156 μM for ClC-K1$_{N68D}$ [solid line in Fig. 2B]), indicating that the presence in position 68 of a neutral residue is much less important for the blocking site of NFA. We conclude that the inhibitory binding site of NFA is quite different from that of 3-phenyl-CPP.

Competition with FFA

The above-described experiments suggest that the blocking site of NFA is different from that of 3-phenyl-CPP, but they do not answer the question of whether the inhibitory binding site and the activating binding site overlap or if they are independent from each other. To study the relationship between the two binding sites, we focused our experiments on ClC-Ka, on which NFA has biphasic behavior. Among the fenamates, FFA is structurally very similar to NFA, the pyridinic ring being substituted with a phenyl ring (Fig. 3A). FFA blocks ClC-Ka currents in a concentration-dependent manner, with a K_d of ~120 μM, whereas it produces an increase of ClC-Kb currents of twofold (Liantonio et al., 2006). To check if FFA and NFA have overlapping binding sites, we performed the following competition experiment. At the fixed concentration of 100 μM FFA, corresponding roughly to the apparent K_d for FFA block, we changed the concentration of NFA in a range that produces only stimulation of ClC-Ka (0, 50, 100, 200 μM). We determined the effect of NFA on the block produced by FFA. A typical experiment is shown in the inset of Figure 3B. As can be seen in Figure 3B, NFA had practically no effect on FFA-induced block, being around 50% at all NFA concentrations. This result strongly suggests that FFA binds to ClC-Ka independently from its occupation by NFA. To corrobate this conclusion, we determined also the effect of FFA on the potentiation of NFA. At a fixed concentration of NFA (200 μM), we changed the concentration of FFA (50, 100, 500 μM). We found that the potentiation produced by 200 μM NFA is not significantly modified by the presence of FFA (Fig. 3C). These results demonstrate that occupation of the activating binding site by NFA does not interfere with FFA-induced block, strongly suggesting the presence of two nonoverlapping fenamate-binding sites.

Competition with Extracellular Chloride Ions

To test for a possible location of the binding site(s) of NFA within the pore, we investigated the dependence of the NFA-induced current activation on the extracellular Cl^- concentration. Applying 50 μM of NFA in high (112 mM) and low (22 mM) extracellular chloride concentrations, we observed only a small variation in effect (Fig. 4). In fact, at high [Cl^-], 50 μM NFA produced an increase of ClC-Ka currents ($I_{drug}/I_{control}$ = 1.87 ± 0.05 at +60 m*V*, $I_{drug}/I_{control}$ = 1.78 ± 0.06 at –100 m*V*), slightly higher than that measured at low [Cl^-] ($I_{drug}/I_{control}$ = 1.63 ± 0.08 at +60 m*V*,

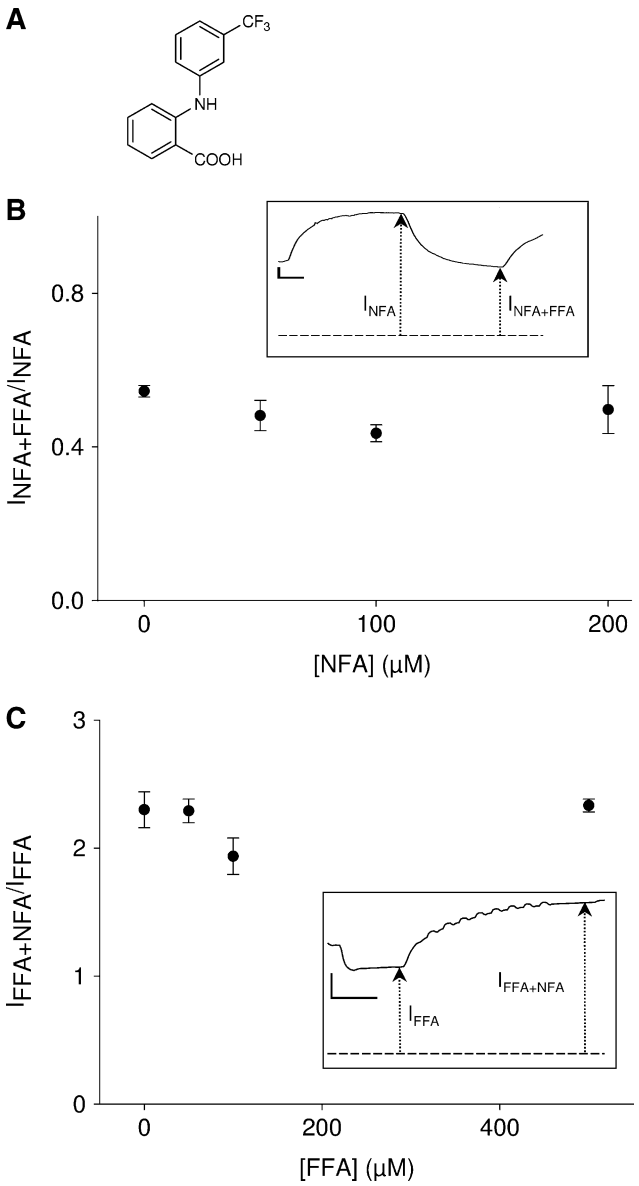

Fig. 3 Lack of competition of NFA and FFA on the human ClC-Ka channel. (**A**) Chemical structure of FFA. (**B**) The block exerted by 100 μM FFA was measured in the additional presence of NFA (50, 100, 200 μM). The block is expressed as the ratio of steady-state currents in the presence of FFA and NFA ($I_{NFA+FFA}$) and the current only in the presence of NFA (I_{NFA}) and is plotted as a function of [NFA]. To illustrate the experimental procedure, the *inset* shows the time course of ClC-Ka currents in a specific experimental condition (100 μM NFA and 100 μM NFA + 100 μM FFA). *Arrows in the insets* indicate the time points at which the indicated current values were obtained. The length of the arrows indicates the size of the corresponding current values. Horizontal scale bar = 50 ms, vertical scale bar = 2 μA. (**C**) Potentiation produced by 200 μM NFA in the additional presence of FFA (50, 100, 500 μM). The potentiation is expressed as the ratio of the current in the presence of NFA and FFA ($I_{NFA+FFA}$) and the current only in the presence of FFA (I_{FFA}) and is plotted as a function of [FFA]. *Inset* shows a typical experiment with 50 μM FFA. Horizontal scale bar = 50 ms, vertical scale bar = 3 μA. The current increase seen after application of 200 μM NFA in the continuous presence of FFA is similar to that seen in the absence of FFA, indicating the independence of the block produced by FFA and the potentiation produced by NFA

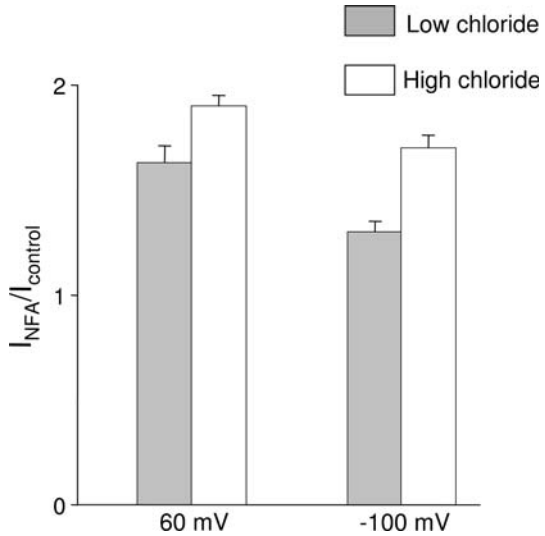

Fig. 4 Extracellular chloride only slightly affects activation of ClC-Ka by NFA. The ratio $I_{NFA}/I_{control}$ is compared at 60 and –100 m*V* measured in 112 mM Cl^- and 22 mM Cl^- using 50 μM NFA. The measurements are from separate oocytes (n = 5 each condition) from the same oocyte batches. The difference at 60 m*V* is marginally significant (p = 0.031, Student's unpaired t-test), whereas the difference at –100 m*V* is significant (p = 0.003, Student's unpaired t-test)

$I_{drug}/I_{control}$ = 1.28 ± 0.08 at –100 m*V*). Clearly, extracellular Cl^- ions do not antagonize the NFA-mediated potentiation, suggesting that the relevant drug-binding site is not located within the pore.

Independence of NFA-Mediated Potentiation of Cyclooxygenase Activity

NFA is a well-known inhibitor of cycloxygenases (Vane & Botting, 1998). To exclude an indirect, cyclooxygenase-mediated mechanism underlying the potentiation of ClC-Ka seen after application of NFA, we tested the effect of indomethacin, a structurally unrelated cyclooxygenase inhibitor (Vane & Botting, 1998). Indomethacin produced a low-affinity block of ClC-Ka with a current reduction of around 29% at 200 μM (Fig. 5A). Fitting the data obtained at 50 and 200 μM (Fig. 5B) with equation 1 (assuming a Hill coefficient of 1) resulted in an apparent K_d for indomethacin of 420 μM (Fig. 5B, solid line). This concentration is well above that needed to block cyclooxygenase activity (Kalgutkar et al., 2000). More importantly, also at lower concentrations (50 μM), no potentiation of ClC-Ka was detected (*data not shown*). Thus, most likely, the NFA-mediated potentiation of ClC-Ka results from a direct interaction with the ClC-Ka/barttin protein complex.

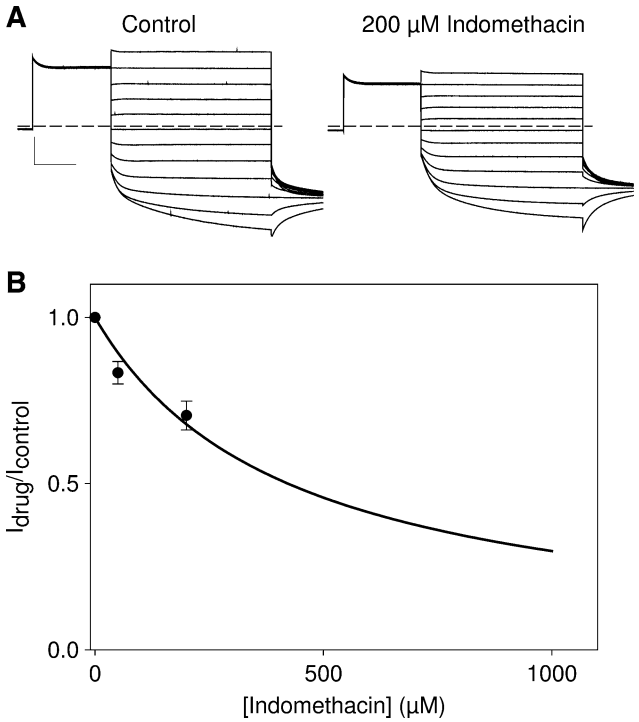

Fig. 5 Low-affinity block of human ClC-Ka produced by indomethacin. (**A**) Representative current recordings are shown in the absence and after application of 200 μM indomethacin. The mean current reduction at 60 mV is about of 30%. Horizontal scale bar = 50 ms, vertical scale bar = 5 µA. (**B**) The ratio of currents in the presence and absence of indomethacin is plotted *vs.* drug concentration. The line is drawn according to the equation $I([\text{indomethacin}])/I_0 = 1/(1 + [\text{indomethacin}]/K_d)$, with an apparent K_d value of 420 μM, which provides the best fit to the data

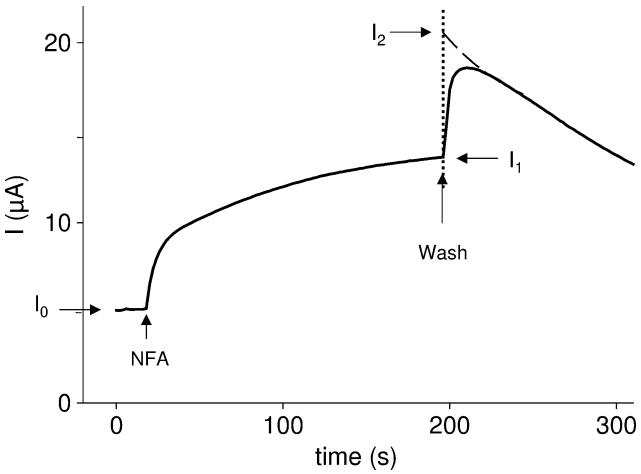

Fig. 6 A perfusion protocol to separate NFA-mediated blocking and potentiation effects. The time course of ClC-Ka currents, measured by applying short pulses to 60 mV every 2 s, is shown. *Vertical arrows* indicate application of 500 μM NFA and washout. *Horizontal arrows* indicate the initial current (I_0), the steady-state current (I_1) after application of 500 μM of NFA and the extrapolated initial current (I_2) after washout. *Dashed line* represents a single-exponential function used to back-extrapolate the decaying current phase to obtain I_2

Separation of NFA-Induced Block and Potentiation of ClC-Ka

To study in more detail the biphasic effect of NFA on ClC-Ka, we applied a particular protocol that allowed us to separate potentiation and block. Later, we will use these results to develop a kinetic model that describes both components. The idea of the protocol is illustrated in Figure 6. We applied a train of 200-ms pulses to 60 mV and plotted the mean current during the 60-mV period as a function of time. The initial current level is indicated by I_0. Applying 500 μM NFA with a fast and continuous perfusion led to a gradual increase of the current to a level denoted I_1 (Fig. 6, arrow). Fast washout of NFA produced an initial enhancement, to an extrapolated level, denoted I_2 (Fig. 6, arrow) and a slower decline to the initial current level. Complete washout of NFA-mediated potentiation required 7–9 min (Liantonio et al., 2006). We interpret the biphasic recovery after washout as follows: the potentiation induced by NFA is probably caused by a slow conformational gating change induced by NFA binding. Washing out NFA immediately relieves channel block, leading to the initial current enhancement, while the conformational effect lasts much longer. Assuming that potentiation and block are independent (an assumption that we will disprove later), the results from the experiment shown in Figure 6 can be formalized in the following way. The initial current is given by

$$I_0 = Nip_o$$

where N is the number of channels, i is the single channel current and p_o is the open probability. We describe the block in terms of the probability of not being blocked, p_u, and the enhancing effect by a potentiation factor, f_p. Thus, the steady-state current with NFA is given by

$$I_1 = Nip_o f_o p_u$$

Assuming that immediately after washout the block is relieved but the potentiation initially persists, the initial current after washout is given by

$$I_2 = Nip_o f_p$$

Thus, we obtain the unblock probability, p_u, by

$$p_u = I_1/I_2$$

and the potentiation factor, f_p, by

$$f_p = I_2/I_o$$

Figure 7A plots p_u as a function of the NFA concentration. The data are clearly not well fitted by a 1:1 binding

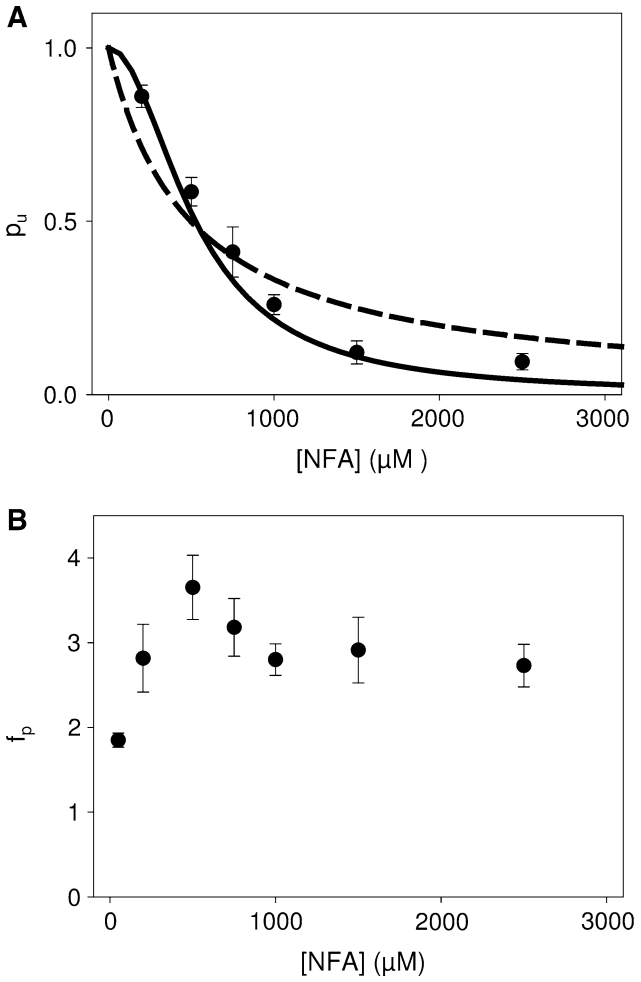

Fig. 7 Block and potentiation mediated by NFA. (**A**) Block produced by NFA, expressed in terms of the unblock probability, p_u, obtained as described in the text, is plotted *vs.* NFA concentration. *Dashed line* is obtained using the Langmuir isotherm equation with a Hill coefficient equal to 1, whereas the *solid line* is drawn using a Hill coefficient equal to 2; in this case, the apparent K_d is 500 μM. (**B**) The potentiation factor, f_p, determined as described in the text, is plotted as a function of NFA concentration

curve (Fig. 7A, dashed line) but are well described by a Langmuir isotherm with a Hill coefficient of about 2 and an apparent K_d of 500 μM (Fig. 7A, solid line). This suggests that two molecules of NFA are needed to block ClC-Ka currents. The potentiation factor, f_p, shows a more complex, biphasic dependence on [NFA] (Fig. 7B). Potentiation has a maximal value of 3.8-fold at 500 μM NFA but decreases again and levels off at a value of 2.7-fold for larger [NFA].

A Quantitative Model to Describe NFA Action

Because NFA is able to increase the open probability by more than a factor of 3, a model that describes the action of NFA has to take gating into account. For simplicity, we assume the presence of only one open and one closed state. Thus, in the absence of NFA the channel is described by $C \longleftrightarrow O$ (Model 0) and the total open probability in the absence of NFA is described by one parameter, p_o. The simplest model, with one NFA-binding site, is thus given by

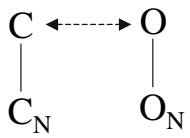

(Model 1)

Because we are interested only in the predictions of the steady-state properties and assuming microscopic reversibility, we cannot determine the connectivity of the model. For this reason, we draw all kinetic models with the minimal number of connections. Model 1 is characterized by two additional parameters, the binding constant of the closed state, K_C, and the binding constant of the open state, K_O. If we assume that state O_N is nonconducting, i.e., blocked, model 1 predicts that NFA can only reduce the current but not enhance it. If, instead, we assume that state O_N is conducting and if $K_O < K_C$, model 1 predicts potentiation but no block at higher [NFA]. If $K_O > K_C$, model 1 predicts only inhibition irrespective of whether O_N is conducting or not. Thus, we need at least one additional binding site:

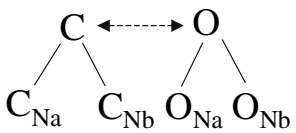

(Model 2)

Model 2 is characterized by four binding constants, K_{Ca}, K_{Cb}, K_{Oa} and K_{Ob}, and the two binding sites (a and b) cannot be simultaneously occupied. As above, both conformationally ''open'' NFA-bound states (i.e., O_{Na} and O_{Nb}) cannot be nonconducting or conducting in order to predict a biphasic concentration-response relationship. Assume that O_{Na} is conducting and O_{Nb} is blocked. The predictions of model 2 for the parameters p_u and f_p, which are operationally defined as illustrated in Figure 6, can be calculated based on the following reasoning. Without NFA, the current is proportional to p_o. In the presence of NFA, in steady state, the current is proportional to $p(O) + p(O_{Na})$, whereas initially after washout of NFA also channels in state O_{Nb} contribute to the current. Thus,

$$p_u = \frac{I_1}{I_2} = \frac{p(O) + p(O_{Na})}{p(O) + p(O_{Na}) + p(O_{Nb})}$$

and

$$f_p = \frac{I_2}{I_0} = \frac{p(O) + p(O_{Na}) + p(O_{Nb})}{p_o}$$

The calculation of the steady-state occupation probabilities of the various states is straightforward. For example, all occupation probabilities can be expressed in terms of $p(O)$. For $p(C)$ we simply have

$$p(C) = \frac{1-p_o}{p_o} p(O)$$

$p(C_{Na})$ can be expressed as

$$p(C_{Na}) = \frac{c}{K_{Ca}} p(C) = \frac{c}{K_{Ca}} \frac{1-p_o}{p_o} p(O)$$

where c is the concentration of NFA. Similar expressions can be found for all other states. Using finally the condition that all occupation probabilities must sum to 1 and inserting the expressions in the above equations for p_u and f_p, we obtain these quantities in terms of the binding constants:

$$p_u = \frac{1 + \frac{c}{K_{Oa}}}{1 + \frac{c}{K_{Oa}} + \frac{c}{K_{Ob}}}$$

and

$$f_p = \frac{1 + \frac{c}{K_{Oa}} + \frac{c}{K_{Ob}}}{p_o\left(1 + \frac{c}{K_{Oa}} + \frac{c}{K_{Ob}}\right) + (1-p_o) + \left(1 + \frac{c}{K_{Ca}} + \frac{c}{K_{Cb}}\right)}$$

However, these equations do not fit our data (*not shown*). As a next step, we thus allowed the simultaneous occupation of both binding sites, resulting in

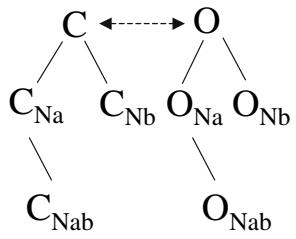

(Model 3)

with two additional binding constants, K_{Cab} and K_{Oab}.

Model 3 provides a reasonable description of our data if, and only if, we assume that states O_{Na} and O_{Nb} are conducting, whereas the channel is blocked when both binding sites are occupied. Very similar to the procedure described above for model 2, we easily obtain expressions for the unblock probability and the potentiation factor for model 3:

$$p_u = \frac{1 + \frac{c}{K_{Oa}} + \frac{c}{K_{Ob}}}{1 + \frac{c}{K_{Oa}} + \frac{c}{K_{Ob}} + \frac{c^2}{K_{Oa}K_{Oab}}} \quad \text{(A)}$$

$$f_p = \frac{1 + \frac{c}{K_{Oa}} + \frac{c}{K_{Ob}} + \frac{c^2}{K_{Oa}K_{Oab}}}{p_O\left(1 + \frac{c}{K_{Oa}} + \frac{c}{K_{Ob}} + \frac{c^2}{K_{Oa}K_{Oab}}\right) + (1-p_O)\left(1 + \frac{c}{K_{Ca}} + \frac{c}{K_{Cb}} + \frac{c^2}{K_{Ca}K_{Cab}}\right)} \quad \text{(B)}$$

The best fit of these equations to the data of Figure 7 is reported in Figure 8 (solid lines). The model provides a good description of the data. As an internal test of consistency, we calculated also the prediction of the model for the direct steady-state concentration-response dependence (given simply by the product $p_u * f_p$; Fig. 8, dashed line). Again, the model is consistent with the experimental data. The parameters obtained from the fit are reported in Table 1. As can be seen from the values, the model predicts that NFA binds to the closed state with lower affinity ($K_{Ca} > K_{Oa}$ and $K_{Cb} > K_{Ob}$). Moreover, for the open channel, the two binding sites have a very different affinity. Clearly, within the model, block and potentiation are not independent from each other. Nevertheless, the operationally defined parameters p_u and f_p contain useful information about the kinetic mechanism. In particular, the unblock probability, p_u, correctly reflects the open channel block in that this parameter is independent from the NFA-binding properties of the closed state.

Discussion

NFA exhibits a complicated, biphasic effect on the kidney Cl^- channel ClC-Ka. Concentrations between 50 and 500 μM of NFA produce an increase of ClC-Ka currents, whereas larger concentrations lead to current block (Liantonio et al., 2006). In contrast, the rat homologue ClC-K1 is simply blocked by NFA in an apparent 1:1 manner. In this report, we have approached several questions regarding the mechanism of NFA action. First of all, we can practically exclude the possibility that the blocking action of NFA is

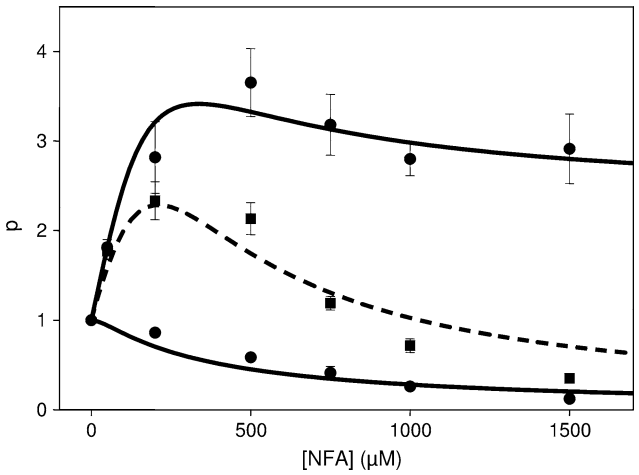

Fig. 8 Predictions of the kinetic model 3. The data obtained with the protocol that allowed us to separate block and potentiation effects (*filled black circles*) were simultaneously fitted using model 3 (*solid line*), resulting in the parameters shown in Table 1. The steady-state NFA concentration-response curve (*filled black squares*) is compared with the predictions of the fit (*dashed line*)

Table 1 Parameters resulting from a best fit of model 3 to the data shown in Figure 8

Parameter	Value
p_o	$2.84 * 10^{-4}$
K_{Oa}	820 μM
K_{Ob}	80 μM
K_{Oab}	42 μM
K_{Ca}	1.8 mM
K_{Cb}	12 mM
K_{Cab}	45 μM

mediated by the same binding site at which 3-phenyl-CPP acts. 3-Phenyl-CPP block is sensitive to extracellular Cl^- and to a point mutation of N68, a residue that points its side chain into the extracellular pore vestibule (Picollo et al., 2004). In contrast, NFA block is almost unaffected by mutating N68 in ClC-K1 (this work) as well as in ClC-Ka (Liantonio et al., 2006). Nevertheless, the slight sensitivity of NFA block to mutations of N68 indicates a certain small influence of the charge at position 68 on NFA block, suggesting that NFA binds at a more external location within the pore.

Even more clearly, our present results show that the NFA site that is responsible for ClC-Ka potentiation is not identical to the 3-phenyl-CPP site and that it is not located deep in the pore. Three lines of evidence support this conclusion. First, NFA potentiation is not influenced by mutating N68 (Liantonio et al., 2006). Second, NFA potentiation is independent of extracellular Cl^-. Third, FFA, a ClC-Ka blocker that binds to the 3-phenyl-CPP site (Liantonio et al., 2006), does not compete with the potentiation mediated by NFA. The finding that NFA does not bind to the previously identified 3-phenyl-CPP site (Picollo et al., 2004) correlates well with the molecular properties of the NFA molecule compared to 3-phenyl-CPP and FFA. According to the modeling studies of Liantonio et al. (2006), NFA has a rigid, coplanar geometry of its aromatic rings. In contrast, 3-phenyl-CPP and FFA are forced to adopt a noncoplanar configuration, likely being thus also more flexible than NFA. Even though also the rings of NFA will rotate at some frequency, we speculate that NFA is too rigid to be easily accommodated in the narrow part of the extracellular vestibule, whereas 3-phenyl-CPP and FFA can reach the deeper binding site.

The third major conclusion that can be drawn from our detailed analysis of NFA action on ClC-Ka is that two NFA molecules can bind to the channel. The model contains several simplifying assumptions. In particular, we assumed the presence of only two gating states. Nevertheless, the model makes several interesting qualitative predictions. The modeling suggests that the two binding sites are not equivalent. Thus, most likely, each protopore of the homodimeric ClC-Ka channel bears two binding sites. The higher-affinity site (site ''b'' in model 3) is mostly responsible for the potentiation of the channel, characterized by a binding constant of 80 μM in the open state. One of the most intriguing features of the model is that block is achieved only if two NFA molecules are bound. The model predicts only a very small positive cooperativity of the two sites in the open state: the binding constants of both sites are roughly twofold smaller if the other site is already occupied. In contrast, in the closed conformation, binding is highly cooperative: binding constants decrease by a factor of around 270 if the other site is occupied. This points to a strong influence of the conformational change on NFA binding.

The ability of NFA to potentiate ClC-Ka (and ClC-Kb) relies on the fact that the open probability of these channels is considerably smaller than 1. The value obtained by our model fitting ($p_o = 2.8 * 10^{-4}$) cannot be considered reliable. In fact, the predictions of the model are almost independent of the exact value of p_o, as long as it is small. For small p_o, equation B is reduced to

$$f_p = \frac{1 + \frac{c}{K_{Oa}} + \frac{c}{K_{Ob}} + \frac{c}{K_{Oa}K_{Oab}}}{1 + \frac{c}{K_{Ca}} + \frac{c}{K_{Cb}} + \frac{c^2}{K_{Ca}+K_{Cab}}}$$

that tends to the limiting value

$$f_p^{\infty} = \frac{K_{Ca}K_{Cab}}{K_{Oa}K_{Oab}}$$

at saturating NFA concentrations. The fact that ClC-Kb is more strongly potentiated by NFA than ClC-Ka (Liantonio

et al., 2006) indicates that, for this channel, the effect of the conformational change on NFA binding is even larger. In contrast, the finding that ClC-K1 is not potentiated by NFA suggests that, for this channel, the gating conformation has little influence on NFA binding. The apparent 1:1 binding in the case of ClC-K1 revealed by the Langmuir isotherm fit suggests either that for this channel binding of one NFA molecule, e.g., to the ''b'' site, is sufficient for block or that the binding constants of the two sites have values such that the block appears to be simpler, clearly a mathematical possibility given by equations A and B.

It is not clear which gating process is affected by NFA. Single-channel measurements are indispensable to find out if NFA alters the open probability of the individual protopores. Alternatively, CLC-K channel open probability may be dominated by a common gate that acts simultaneously on both pores of the double-barreled channel, in analogy to the slow gate of the ClC-0 channel (Pusch & Jentsch, 2005).

It will be highly interesting to identify the amino acids that are involved in the NFA binding sites. This may allow a better understanding of the molecular mechanism of NFA-mediated potentiation and the development of higher-affinity potentiators. Such drugs are of considerable medical potential, e.g., for the treatment of Bartter's syndrome type III.

Acknowledgement We thank T. Jentsch for providing all cDNA clones, M. De Bellis for help in molecular biology and G. Gaggero for help in constructing the recording chamber. The financial support of Telethon Italy (grant GGP04018) is gratefully acknowledged.

References

Adachi S, Uchida S, Ito H, Hata M, Hiroe M, Marumo F, Sasaki S (1994) Two isoforms of a chloride channel predominantly expressed in thick ascending limb of Henle's loop and collecting ducts of rat kidney. J Biol Chem 269:17677–17683

Birkenhäger R, Otto E, Schurmann MJ, Vollmer M, Ruf EM, Maier-Lutz I, Beekmann F, Fekete A, Omran H, Feldmann D, Milford DV, Jeck N, Konrad M, Landau D, Knoers NV, Antignac C, Sudbrak R, Kispert A, Hildebrandt F (2001) Mutation of BSND causes Bartter syndrome with sensorineural deafness and kidney failure. Nat Genet 29:310–314

Brandt S, Jentsch TJ (1995) ClC-6 and ClC-7 are two novel broadly expressed members of the CLC chloride channel family. FEBS Lett 377:15–20

Estévez R, Boettger T, Stein V, Birkenhäger R, Otto E, Hildebrandt F, Jentsch TJ (2001) Barttin is a Cl^- channel beta-subunit crucial for renal Cl^- reabsorption and inner ear K^+ secretion. Nature 414:558–561

Fong P (2004) CLC-K channels: if the drug fits, use it. EMBO Rep 5:565–566

Gögelein H, Dahlem D, Englert HC, Lang HJ (1990) Flufenamic acid, mefenamic acid and niflumic acid inhibit single nonselective cation channels in the rat exocrine pancreas. FEBS Lett 268:79–82

Kalgutkar AS, Crews BC, Rowlinson SW, Marnett AB, Kozak KR, Remmel RP, Marnett LJ (2000) Biochemically based design of cyclooxygenase-2 (COX-2) inhibitors: facile conversion of nonsteroidal antiinflammatory drugs to potent and highly selective COX-2 inhibitors. Proc Natl Acad Sci USA 97:925–930

Kieferle S, Fong P, Bens M, Vandewalle A, Jentsch TJ (1994) Two highly homologous members of the ClC chloride channel family in both rat and human kidney. Proc Natl Acad Sci USA 91:6943–6947

Lee YT, Wang Q (1999) Inhibition of hKv2.1, a major human neuronal voltage-gated K^+ channel, by meclofenamic acid. Eur J Pharmacol 378:349–356

Liantonio A, Picollo A, Babini E, Carbonara G, Fracchiolla G, Loiodice F, Tortorella V, Pusch M, Camerino DC (2006) Activation and inhibition of kidney CLC-K chloride channels by fenamates. Mol Pharmacol 69:165–173

Liantonio A, Pusch M, Picollo A, Guida P, De Luca A, Pierno S, Fracchiolla G, Loiodice F, Tortorella P, Conte Camerino D (2004) Investigations of pharmacologic properties of the renal CLC-K1 chloride channel co-expressed with barttin by the use of 2-(*p*-chlorophenoxy)propionic acid derivatives and other structurally unrelated chloride channels blockers. J Am Soc Nephrol 15:13–20

Matsumura Y, Uchida S, Kondo Y, Miyazaki H, Ko SB, Hayama A, Morimoto T, Liu W, Arisawa M, Sasaki S, Marumo F (1999) Overt nephrogenic diabetes insipidus in mice lacking the CLC-K1 chloride channel. Nat Genet 21:95–98

McCarty NA, McDonough S, Cohen BN, Riordan JR, Davidson N, Lester HA (1993) Voltage-dependent block of the cystic fibrosis transmembrane conductance regulator Cl^- channel by two closely related arylaminobenzoates. J Gen Physiol 102:1–23

Picollo A, Liantonio A, Didonna MP, Elia L, Camerino DC, Pusch M (2004) Molecular determinants of differential pore blocking of kidney CLC-K chloride channels. EMBO Rep 5:584–589

Pusch M, Jentsch TJ (2005) Unique structure and function of chloride transporting CLC proteins. IEEE Trans Nanobiosci 4:49–57

Pusch M, Liantonio A, Bertorello L, Accardi A, De Luca A, Pierno S, Tortorella V, Camerino DC (2000) Pharmacological characterization of chloride channels belonging to the ClC family by the use of chiral clofibric acid derivatives. Mol Pharmacol 58:498–507

Qu Z, Hartzell HC (2000) Anion permeation in Ca^{2+}-activated Cl^- channels. J Gen Physiol 116:825–844

Simon DB, Bindra RS, Mansfield TA, Nelson-Williams C, Mendonca E, Stone R, Schurman S, Nayir A, Alpay H, Bakkaloglu A, Rodriguez-Soriano J, Morales JM, Sanjad SA, Taylor CM, Pilz D, Brem A, Trachtman H, Griswold W, Richard GA, John E, Lifton RP (1997) Mutations in the chloride channel gene, *CLCNKB*, cause Bartter's syndrome type III. Nat Genet 17:171–178

Uchida S, Sasaki S (2005) Function of chloride channels in the kidney. Annu Rev Physiol 67:759–778

Vandewalle A, Cluzeaud F, Bens M, Kieferle S, Steinmeyer K, Jentsch TJ (1997) Localization and induction by dehydration of ClC-K chloride channels in the rat kidney. Am J Physiol 272:F678–F688

Vane JR, Botting RM (1998) Mechanism of action of nonsteroidal anti-inflammatory drugs. Am J Med 104:2S–8S, discussion 21S–22S

White MM, Aylwin M (1990) Niflumic and flufenamic acids are potent reversible blockers of Ca^{2+}-activated Cl^- channels in *Xenopus* oocytes. Mol Pharmacol 37:720–724